Development 138, 3955-3966 (2011) doi:10.1242/dev.059063

Knockdown of embryonic myosin heavy chain reveals an essential role in the morphology and function of the developing heart

Catrin Sian Rutland[1,2], Luis Polo-Parada[3], Elisabeth Ehler[4], Aziza Alibhai[1], Aaran Thorpe[1], Suganthi Suren[5], Richard D. Emes[2], Bhakti Patel[1] and Siobhan Loughna[1,*]

SUMMARY

The expression and function of embryonic myosin heavy chain (eMYH) has not been investigated within the early developing heart. This is despite the knowledge that other structural proteins, such as alpha and beta myosin heavy chains and cardiac alpha actin, play crucial roles in atrial septal development and cardiac function. Most cases of atrial septal defects and cardiomyopathy are not associated with a known causative gene, suggesting that further analysis into candidate genes is required. Expression studies localised eMYH in the developing chick heart. eMYH knockdown was achieved using morpholinos in a temporal manner and functional studies were carried out using electrical and calcium signalling methodologies. Knockdown in the early embryo led to abnormal atrial septal development and heart enlargement. Intriguingly, action potentials of the eMYH knockdown hearts were abnormal in comparison with the alpha and beta myosin heavy chain knockdowns and controls. Although myofibrillogenesis appeared normal, in knockdown hearts the tissue integrity was affected owing to apparent focal points of myocyte loss and an increase in cell death. An expression profile of human skeletal myosin heavy chain genes suggests that human myosin heavy chain 3 is the functional homologue of the chick eMYH gene. These data provide compelling evidence that eMYH plays a crucial role in important processes in the early developing heart and, hence, is a candidate causative gene for atrial septal defects and cardiomyopathy.

KEY WORDS: Atrial septal development, Cardiomyopathy, Myosin, Chick

INTRODUCTION

Myosin heavy chain isoforms are traditionally known to be major structural components of the heart muscle contractile apparatus. The myocardia of the atrial and ventricular chambers differ in their contractile and electrophysiological properties, which are partly determined by the expression of certain genes. In humans and chick, the 'cardiac' myosin heavy chain genes, alpha *MYH* (α*MYH* or atrial *MYH*) and beta *MYH* (β*MYH* or ventricular *MYH*), are located on separate chromosomes, whereas the 'skeletal' MYH genes are clustered together on the same chromosome. During development and in the adult, αMYH is predominately expressed in the atrial chamber and βMYH in the ventricular chamber in both humans and chicks (Oana et al., 1998; Reiser et al., 2001; Somi et al., 2006; Wessels et al., 2000; Wessels et al., 1991). Of the skeletal genes, four are expressed in the heart in the chicken. Neonatal fast, slow skeletal and slow tonic MYH are predominately expressed in the heart conductive cells (Gonzalez-Sanchez and Bader, 1985; Machida et al., 2000; Machida et al., 2002). Although embryonic MYH (eMYH) has been shown to be expressed in the myotome, skeletal muscle and chick heart late in development (from day 12) (Gulick et al., 1987; Lagrutta et al., 1989; Lyons et al., 1990; Merrifield et al., 1989; Sacks et al., 2003), expression during early cardiogenesis has not been determined. To our knowledge, none of the skeletal MYH genes is known to be expressed in the human heart.

Looping of the primitive heart tube is initiated from Hamburger and Hamilton stage (HH) 10 (during day 2) in the chick (Hamburger and Hamilton, 1951; Sissman, 1970). This tube is subsequently divided into chambers by the formation of septa, a process initiated in the primitive single atrium from the dorsocranial wall at ~HH14 (Hendrix and Morse, 1977; Morse, 1978; Quiring, 1933). This septum primum extends into the chamber and ultimately fuses with endocardial cushions, dividing the heart into left and right atrial chambers. In humans, atrial septal defects (ASDs) occur in approximately 1 in 1500 live births. The molecular genetics of ASDs are being elucidated with mutations found in a number of genes, including the transcription factors *Nkx2.5*, *Tbx5* and *Gata4*, and the structural proteins *MYH6*, *MYH7* and alpha cardiac actin (Wessels and Willems, 2010). Although these mutations have provided important insights into cardiac morphogenesis and ASD formation, in many families and individuals the causative gene is still unknown.

Cardiomyopathies are contractile diseases of the heart that are associated with heart enlargement and dysfunction. The two most common types are hypertrophic and dilated cardiomyopathy (CM).

[1]School of Biomedical Sciences, University of Nottingham, Queens Medical Centre, Derby Road, Nottingham, NG7 2UH, UK. [2]School of Veterinary Medicine and Science, University of Nottingham, Sutton Bonington Campus, Sutton Bonington, Leicestershire, LE12 5RD, UK. [3]Department of Medical Pharmacology and Physiology, School of Medicine, University of Missouri, Dalton Cardiovascular Research Center, 134 Research Park, Columbia MO. 65211, USA. [4]Randall Division of Cell and Molecular Biophysics and The Cardiovascular Division, New Hunt's House, King's College London, Guy's Campus, London, SE1 1UL, UK. [5]Human Developmental Biology Resource, Neural Development Unit, UCL Institute of Child Health, 30 Guilford Street, London, WC1N 1EH, UK.

*Author for correspondence (siobhan.loughna@nottingham.ac.uk)

Accepted 30 June 2011

Hypertrophic CM (HCM) is defined as the unexplained presence of a notable thickening of the ventricular wall and dilated CM (DCM) is defined by ventricular dilatation and decreased contractile function (Maron et al., 2006). Mutations in a range of human sarcomeric genes have been associated with both HCM and DCM, including *MYH6* (human homologue of α*MYH*) and *MYH7* (human homologue of β*MYH*) (Carniel et al., 2005; Niimura et al., 2002; Walsh et al., 2010). It is also of note that children can be afflicted with cardiomyopathy (Towbin et al., 2006). Interestingly, mutations in the structural proteins MYH6, MYH7 and alpha cardiac actin have been associated with cardiomyopathy and ASDs in humans (Budde et al., 2007; Carniel et al., 2005; Ching et al., 2005; Matsson et al., 2008; Mogensen et al., 2004; Monserrat et al., 2007; Olson et al., 1998).

Although *eMYH* was isolated and sequenced in 1987 (Molina et al., 1987), little has been done to describe its role during heart development. We describe here that eMYH is present in the early developing heart and that upon knockdown during early cardiogenesis, the atrial septa developed abnormally. In addition, the hearts had ventricular DCM and disrupted trabeculae development, and most ventricular cardiomyocytes were either electrically inactive or abnormalities in electrical activities were observed. Although the sarcomeres appeared normal, tissue integrity was compromised and apoptosis levels were increased. These data suggest that the structural protein eMYH is a candidate gene for ASDs and DCM, and is crucial for normal contractile function.

MATERIALS AND METHODS

Morpholino design

Two morpholinos were designed against *eMYH* (accession number J02714) (Molina et al., 1987): 5′-TCAGCATCTGTAGCCATCGTCGCT-3′ (first experimental designed to translational start site) and 5′-TTATTGGGAGTAATGCAGCAAGTAT-3′ (second experimental designed upstream of start site). A 5 base pair (bp) mismatch (indicated in lower case) negative control morpholino (5′-TCAcCATCTcTAcCCATCcTCcCT-3′) and a GeneTools standard control (SC) morpholino (to mutated human beta-globin gene; 5′-CCTCTTACCTCAGTTACAATTTATA-3′) were used. An α*MYH* morpholino was used as described previously (Rutland et al., 2009). A translational start site morpholino for β*MYH* (5′-CCGTCATGTCCATCATCTTGGCAAG-3′) was designed. Morpholinos were fluorescein or lissamine tagged (GeneTools LLC, USA) and underwent strict sequence similarity testing to ensure gene specificity.

eMYH knockdown

Knockdown was performed as previously described (Rutland et al., 2009) using fertile chicken eggs (*Gallus gallus*; Henry Stewart, UK) at HH12, HH14 or HH16 (Hamburger and Hamilton, 1951), equivalent to 50, 54 and 57 hours incubation, respectively. Studies were performed within national (UK Home Office) and institutional ethical regulations. When determining the optimal concentration of eMYH morpholino, 125 μM, 250 μM or 500 μM were achieved by resuspension in equal amounts of 30% F127 pluronic gel (BASF Corporation, Germany) and HBSS. The phenotype was found to be mild at 125 μM, and obvious at 250 μM or 500 μM. Non-specific effects were not observed at any concentration. As there were no phenotypic differences between hearts knocked down with 250 μM or 500 μM, 250 μM was used for all further studies. The first and second eMYH morpholinos gave the same phenotype with a similar penetrance, therefore embryo numbers pertain to both experimental morpholino groups pooled. Mismatch, SC and untreated control groups were pooled with a minimum of three embryos per control type, per developmental stage. Age-matched ‘untreated’ control embryos were opened at the same stage as other embryos but morpholino/pluronic gel was not applied. HH14/19 represents knockdown at HH14, harvesting at HH19; similar abbreviations were used for all knockdown and harvesting stages.

Embryo isolation

Embryos were harvested using a fluorescent SV11 stereomicroscope (Zeiss, Germany) to determine morpholino uptake, stage embryos, count somites and perform external phenotypic analysis (Bellairs and Osmond, 1998; Hamburger and Hamilton, 1951). Data showing the numbers of chick embryos alive at harvesting (HH19; 81 hours) and those that were ‘morpholino positive’ were collected from 250 μM experiments and statistically analysed (see below); n=356 untreated, 164 SC, 38 eMYH mismatch and 360 eMYH knockdown embryos.

Bioinformatics

To determine possible homologous relationships between human and chicken MYH clusters, genomic DNA encompassing the identified cluster on chicken chromosome 18 (genome.cse.ucsc.edu, coordinates *G. gallus* build 18 positions 1-1768914) and the six known human swissprot proteins (P35580.3, P11055.3, P13535.3, Q9UKX2.1, P12882.3, Q9Y623.2, Q9UKX3.1) were used to predict all myosin-like genes in this region using exonerate (Slater and Birney, 2005). Mouse, human and chicken MYH genes showed large regions of conservation and clustering, although orthology could not be determined. Translations of predicted genes were aligned to the human proteins using muscle (Edgar, 2004) to produce a phylogenetic tree (Guindon and Gascuel, 2003). Analysis of known and predicted MYH genes revealed a single human-chicken orthologue of *MYH13* and lineage-specific duplications of MYH genes in the chicken genome. The addition of identified MYH genes from the anole lizard (*Anolis carolinensis*) and zebrafinch (*Taeniopygia guttata*) confirmed that these expansions are largely avian specific, suggesting that at the point of divergence of the diapsids (birds, lizards) and synapsids (mammals) a small MYH gene family existed. Following the divergence of lizard and birds the independent expansion of avian and mammalian MYH genes began. In these examples of out-paralogue expansions it is not advisable to computationally infer specific function to single genes, hence RNA expression studies were performed.

RNA expression

RNA was extracted from chick HH12, 14, 16, 19, 22, 24 and 26 hearts, and human 7-week foetal heart and 8-week skeletal muscle using RNeasy Micro and Midi Kits (Qiagen, UK). Commercial RNAs used were: human foetal skeletal muscle (19 weeks; AMS Biotechnology, UK) and human adult skeletal muscle, human adult heart and human foetal heart (12-31 weeks pooled samples; Clontech, USA). Reverse transcription reactions were performed using random primers with SuperScript III Reverse Transcriptase (Invitrogen, UK), and 1 μg of RNA per reaction. PCR reactions: 95°C for 4 minutes, then 35 cycles of 94°C for 30 seconds, 56°C for 30 seconds, 72°C for 1 minute for all primers except actin and eMYH which required annealing at 60°C. Primers were designed to chick *eMYH*, 5′-GCCAAGGCAAATTTAGAGAAGA-3′ and 5′-TCATTAATGGTGCGCTGTTG-3′ (95 bp RT-PCR product); human *MYH1*, 5′-CTGGCTCTCCTCTTTGTTGG-3′ and 5′-GAGAGCAGACACAGTCTGGAAA-3′ (105 bp); human *MYH2*, 5′-GGAGAGGGAGCTGGTGGA-3′ and 5′-CTCTCTGAAAAGGGCAGACA-3′ (84 bp); human *MYH3*, 5′-AAATGGAAGTGTTCGGCATA-3′ and 5′-GGCGTACACATCCTCTGGTT-3′ (221 bp); human *MYH4*, 5′-GGACCAGCTTAGTGAAATAAAAACA-3′ and 5′-TCGGGATAGCTGAGAAACCA-3′ (151 bp); human *MYH8*, 5′-TCTTCTGGAAGAAATGAGAGATGA-3′ and 5′-GCTTCTCTCCTTTGCAACATC-3′ (117 bp); human *MYH13*, 5′-CGAGGCTCAAAATCGTCCA-3′ and 5′-AGAGTGAGCATCCGGTCATC-3′ (141 bp); human β-actin, 5′-CCTGGCACCCAGCACAAT-3′ and 5′-GGCGATCCACACGGAGTACT-3′ (60 bp) (kindly provided by Dr Andy Bennett, University of Nottingham). All primers spanned an intron. Products were resolved on 1.5% agarose gels against Hyperladder IV (Bioline, UK). Amplicons were cloned and sequenced (Biopolymer Synthesis and Analysis Unit, University of Nottingham).

For in situ hybridization, human and mouse embryos were fixed in 4% paraformaldehyde (PFA) in phosphate-buffered saline (PBS) overnight at 4°C, followed by dehydration, paraffin wax embedding and cutting of 8-μm-thick sections. Proteins were removed using proteinase K (20 mg/ml) in PBS. A 221 bp PCR product of human *MYH3* (NM_002470.2, 94-315

bp) was ligated into pGEM-T (Promega) and used on both human and mouse tissue. Antisense and sense probes were prepared by linearising plasmids with *Apa*I and *Sal*I, respectively. Digoxigenin (DIG)-UTP was incorporated into riboprobes during in vitro transcription using DIG RNA Labelling Mix (Roche) according to manufacturer's instructions. Antisense and sense probes were generated using SP6 and T7 polymerase, respectively. The remainder of the in situ hybridization procedure was as previously described (Kelberman et al., 2008).

Western blotting

Three HH19 hearts per 'sample' were dissected, snap frozen in liquid nitrogen and stored at –80°C. Samples were resolved by SDS-PAGE gels as previously described (Rutland et al., 2009) with 1 hour at room temperature (RT) incubation with EB165 [eMYH; 1:500; Developmental Studies Hybridoma Bank (DSHB), USA] (Cerny and Bandman, 1987) or glyceraldehyde 3-phosphate dehydrogenase (GAPDH; loading control; 1:1000; Abcam, UK), followed by 1 hour at RT with a mouse monoclonal secondary antibody (Dako, Denmark). Immunoblots containing untreated, SC and knockdown heart samples were performed in triplicate using different samples and blots each time.

Phenotypic and immunohistochemical studies

Untreated control embryos were isolated at HH12, 14, 16, 19, 22, 24 and 26, fixed in 4% PFA, washed in 1× PBS, dehydrated in an ethanol series and wax embedded in a transverse orientation. Serial 8 μm sections were taken (DSC1 microtome, Leica, Germany), dewaxed, rehydrated and stained with Mayers haemalum (Raymond Lamb, UK) or used for immunohistochemistry (see below). Unless otherwise stated, morphological analysis was performed double blind using an Axioskop 2 microscope (Zeiss, USA).

Immunohistochemistry

After tissue rehydration, antigen unmasking was performed (microwaving for 10 minutes in 10 mM sodium citrate, pH 6.0). An avidin-biotin phosphatase amplification kit (StreptABComplex Duet Kit; Dako, Denmark) was used according to manufacturer's instructions including a 1 hour EB165 antibody incubation (1:50 eMYH; DSHB, USA) (Cerny and Bandman, 1987) and counterstaining in Mayers haemalum (Raymond Lamb, UK).

Alternatively, sections were subjected to 5 minute treatments of 3% acetic acid (pH 2.5) and 1% Alcian Blue/acetic acid, 10 minutes in 50% periodic acid solution, followed by 15 minutes in Schiff's reagent before ethanol dehydration.

Systematic random sampling

Systematic random sampling (Mayhew, 1991) was used to assess tissue proportions throughout HH14/19 hearts [control (untreated, mismatch and SC) and eMYH; n=9 per group]. A 96-point grid was placed over every third section throughout the heart, tissue type on each point was identified (6879 points counted) and average tissue proportions were calculated and tested for statistical significance (see below). Identical procedures were used for HH14/17 chicks (n=14 control, n=16 eMYH knockdown; 7961 points counted).

Proliferation and apoptosis

Embryo isolation and processing methods were employed at HH14/19 (as above) and cells visualised using a proliferating cell nuclear antigen (PCNA) staining kit using the manufacturer's instructions to indicate cell proliferation (Zymed Laboratories, USA). Alternatively, embryos were placed into 30% sucrose for 30 minutes, orientated in OCT and frozen using liquid nitrogen-cooled isopentane. Serial sections were cut (20 μM), mounted, fixed for 3 minutes in 4% PFA and an 'in situ Cell Death Detection Kit' (Roche Diagnostics, Germany) used to indicate apoptotic cells in accordance with manufacturer's instructions. Systematic random sampling (Mayhew, 1991) was utilised to count positive cells against total cell count in the ventricle, atrium and septum (minimum of n=3 per eMYH knockdown and control hearts) to calculate proportions of proliferating/apoptotic cells for statistical analysis (see below).

Immunofluorescence and electron microscopy

Hearts from PFA-fixed chick embryos were dissected and immersed in 1 mg/ml hyaluronidase (Sigma) in PBS for 1 hour at RT, with permeabilisation in 0.2% Triton X-100/PBS (PBT) for 45 min and blocked with 5% preimmune goat serum in 1% BSA/TBS for 30 min at RT with primary antibody incubations overnight at 4°C. Hearts were washed six times for 20 minutes in 0.002% PBT, incubated with secondary antibody either overnight at 4°C or for 6 hours at RT, washed six times for 20 minutes each wash in PBT and mounted for confocal microscopy. For immunostaining with EB165 (eMYH; DSHB), hearts were dissected, fixed overnight in 90% methanol/10% DMSO at –20°C, rehydrated in PBS and immersed in 1 mg/ml hyaluronidase for 1 hour at RT. Blocking steps and subsequent antibody incubations were carried out as above and counterstained using an antibody against sarcomeric alpha-actinin (Ehler et al., 1999).

Analysis was carried out using a Zeiss (Germany) 510 confocal microscope equipped with 405 diode, argon and helium neon lasers using a 63×/NA1.4 oil immersion objective. Data were processed in Image J (NIH, USA). Antibodies used were: mouse anti-sarcomeric alpha-actinin (Sigma, UK), rabbit anti beta-catenin (Sigma, UK), rabbit anti EH-myomesin (Agarkova et al., 2000), rabbit anti-MyBP-C (Ahuja et al., 2004), Cy2- or Cy5-conjugated anti-rabbit immunoglobulins and Cy3- or Cy5-conjugated anti-mouse immunoglobulins (Jackson Immunochemicals, USA). DAPI was purchased from Sigma (UK). Combinations of Cy2 and Cy5 were used for lissamine and Cy3 and Cy5 for fluorescein-tagged morpholinos.

Hearts undergoing transmission electron microscopy (n=5 eMYH knockdown, 5 control) were fixed, sectioned (0.5 μm) and visualised using a FEI Tecnai 12 Biotwin TEM at 4000-43,000× magnification.

Electrical activity and calcium signalling

Knockdown embryos (HH14/19; α-, β- or eMYH morpholinos) were utilised for intracellular recordings of the electrical responses of heart cells. Glass micropipettes (Sutter Instruments, USA) were pulled with a P-97 Flaming/Brown micropipette puller (Sutter Instruments, USA),filled with 3M KCl and connected to a Bridge Amplifier BA-1S (npi-Tamm, Germany); a resistance of 60-80 MΩ was used. Recordings were displayed on an oscilloscope (Instek, USA), digitised in parallel, and stored and processed via Digidata 1440A with Axotape 10 Software (Molecular Devices, USA).

Action potentials were classified on the maximal rate of rise (dV/dt_{max}), action potential duration (APD) (APD_{50} and APD_{90} measured at 50% or 90% repolarization, respectively), amplitude, prominence of phase 4 depolarization, maximal diastolic potential and resting membrane potential. For evaluation of Ca^{2+} transients, single cell cultures were incubated 2-3 hours post-plating with 1 μM Fluoro-5 FF-AM (Invitrogen, USA) or Rhod-2 AM (Anaspec, USA) (green and red fluorescent Ca^{2+} sensitive dyes, respectively) for 10-15 minutes. Changes in intracellular Ca^{2+} were detected by monitoring fluorescent dye intensity changes. Cell culture dishes were mounted in a temperate controller on an inverted microscope IX71 (Olympus, UK) using the appropriate excitation and emission filter set (Semrock, USA). Fluorescent signal was monitored using a photomultiplier (PTI, USA) coupled with an A/D digitiser and displayed as ΔF/Fo. n=16 per MYH tested. The cardiomyocytes with no spontaneous contraction in vitro were positive for Calcein-AM staining (cell viability test) and negative for propidium iodine staining (membrane integrity test).

Patch clamp recordings

Standard whole-cell patch clamp configuration, including solutions and voltage protocols, was as previously described (Davies et al., 1996; Hamill et al., 1981; Wang and Duff, 1997). An EPC 10 amplifier under the control and measuring of Patch Master (Heka Instruments) was used. RSeries resistance was 0.5-3.0 MΩ (mean 1.6±0.2 MΩ) and membrane capacitance was 3.8-4.9 pF (mean 5.1±0.6 pF).

Statistics

Levene's test for equality of variances followed by t-test for equality of means or Analysis of Variance (ANOVA) with post-hoc testing for multiple groups on SPSS V17 (SPSS, USA) were used; $P<0.05$ was considered to be significant.

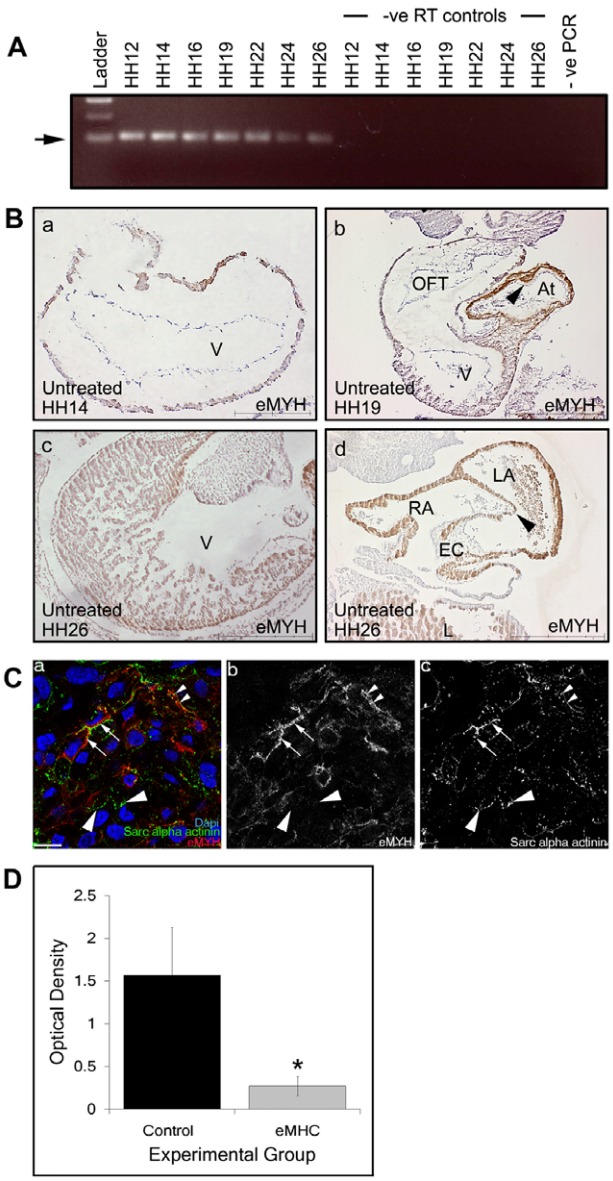

Fig. 1. eMYH is expressed during chick cardiogenesis and is knocked down upon morpholino application. (**A**) mRNA expression was present in HH12, 14, 16, 19, 22, 24 and 26 embryonic heart tissue (arrow). No signal was observed in negative (–ve) RT and –ve PCR controls. (**B**) eMYH was found throughout the HH14 heart wall (**a**), outflow tract (OFT), atrium (At), atrial septa (arrowhead) and, to a lesser extent, HH19 ventricular (V) myocardium and trabeculae (**b**). At HH26 (**c**,**d**), staining was seen in the ventricle, left and right atria (LA and RA, respectively) and atrial septa. Endocardial cushion (EC) staining was absent. Scale bars: 200 μm in a; 500 μm in b-d. L, liver. (**C**) Confocal micrographs show eMYH staining (**a**,**b**), particularly associated with plasma membranes (small arrowheads), A-bands of emerging myofibrils (arrows) but not in all myofibrils (large arrowheads) compared with sarcomeric alpha actinin (a,**c**). Scale bar: 10 μm. DAPI labels nuclei blue. (**D**) Western analysis demonstrated an optical density of 0.27 (eMYH knockdown) and 1.57 (control). *P<0.02. Error bars represent s.e.m.

RESULTS

eMYH is expressed during early cardiogenesis

RNA expression profiling showed that eMYH was present in chick heart at all stages analysed (HH12-26) (Fig. 1A). At HH14, immunohistochemical eMYH (EB165)-positive staining was seen throughout the myocardial wall (Fig. 1Ba). Intense expression was seen throughout the outflow tract (OFT), myocardium of the atrial ventricular canal (AVC) and atrial myocardial walls at HH19-26 (Fig. 1Bb,d). In addition, eMYH staining was identified in the atrial septum, as it extended into the atrial chamber and persisted once it had fused with negatively stained endocardial cushions (Fig. 1B). Lower levels of staining were present throughout the ventricular myocardial walls and trabeculae (Fig. 1Bb,c). Expression of eMYH was also observed within the sinus venosus of the heart and myotome-derived premuscle masses (data not shown). As shown in Fig. S1C,F in the supplementary material, eMYH expression was localised to the heart tube and confocal microscopy analysis revealed that eMYH was expressed by a subset of cardiomyocytes and localised close to the plasma membrane (small arrowheads in Fig. 1C). In a subset of cardiomyocyte myofibrils that express eMYH, localisation to the A-bands was seen (arrows in Fig. 1C), as judged by counterstaining for the Z-disc protein sarcomeric alpha-actinin. To determine whether eMYH expression can be correlated with cardiomyocyte populations originating from the primary or secondary heart field, eMYH was localised in early heart whole-mount preparations. At all developmental stages analysed (7, 8 and 12 somites, equivalent to HH9 to early HH11), eMYH was restricted to the heart itself, but was not expressed homogeneously (see Fig. S1 in the supplementary material). More eMYH-positive cells were detected caudally in the heart at all stages, but the area of expression was too broad for a strict correlation with secondary heart field populations.

Validation of controls and survival rates of embryos

All of the control embryos analysed both internally and externally (n=83) had normal phenotypes, except for one untreated control embryo in the HH16 control group (1/13), which had a comparatively small heart and septum. As a small heart and septum was not seen in any other control embryo it was presumed to be due to developmental variation.

Data from untreated embryos (n=356) collected at HH19 showed a survival rate of 86.2%, SC embryos (n=164) 83.5%, eMYH mismatch knockdown (n=38) 89.4% and those receiving eMYH morpholino (n=360) a rate of 83.3% (no significant differences, P=0.9). Those identified as ‘morpholino positive’ (determined by the level of fluorescence), totalled 60.6% of SCs, 47.1% of eMYH mismatch and 60% of eMYH knockdown embryos (no significant differences, P=0.7). Knockdown and survival rates for the αMYH knockdown hearts (n=203) were as previously published (Rutland et al., 2009). Survival rate for βMYH knockdown embryos (n=47) was 81% and morpholino uptake 60%. We have previously demonstrated that knockdown of chick αMYH leads to abnormal atrial septal development (Ching et al., 2005; Rutland et al., 2009), whereas knockdown of βMYH causes heart enlargement but atrial septal development was normal (C.S.R., A.A., A.T. and S.L., unpublished data).

Knockdown of eMYH leads to dilated cardiomyopathy

Analysis of eMYH protein level showed a significant reduction of 82.6% (P=0.02) in knockdown hearts compared with control hearts (Fig. 1D). Ventricular size was analysed externally when harvesting and upon internal phenotypic analysis (Table 1). The samples below pertain only to those that underwent both comparisons.

Table 1. Summary of embryos with abnormal phenotype to the ventricular chamber

			Ventricle of heart*		Trabeculation*	
Stage†	Embryo type‡	Total	Enlarged	Normal	Reduced	Normal
HH12/19	Control	12	0	12	0	12
	eMYH knockdown	10	7	3	10	0
HH14/19	Control	58	0	58	0	58
	eMYH knockdown	43	38	5	42	1
HH16/19	Control	13§	0	13	0	13
	eMYH knockdown	8	5	3	8	0

*Assessment of ventricular size and degree of trabeculation based on qualitative analysis of either gross morphological features (ventricle) or histological serial sections (trabeculae).
†Stage of development when knockdown/harvesting were performed.
‡Control embryos include standard control, mismatch and untreated; eMYH denotes embryonic myosin heavy chain.
§One out of a total of 13 embryos had a small heart and a reduced septum.

Following HH12/19 knockdown, it was noted that 7 of 10 embryos had enlarged ventricular chambers (70%) compared with controls (0/12; Fig. 2B compared with 2A). This external phenotype was also present following knockdown at HH14/19 (38/43 or 88%; Fig. 2D compared with 2C) and HH16/19 (5/8 or 62.5%) and was confirmed upon internal phenotypic analysis. Stereology showed knockdown hearts were 26% larger than controls (P=0.05). None of the control embryos had an enlarged ventricular chamber (0/83; Fig. 2A,C).

Trabeculae can be observed from about HH17, with distinct structures by HH19 (Ben-Shachar et al., 1985; Sedmera et al., 1997). In HH14/17 hearts, trabeculae could not be distinguished and no stereological differences in ventricular size were observed (P>0.05; n=14 control, n=16 eMYH knockdowns). By contrast, internal phenotypic analysis of HH19 knockdowns showed ventricular dilation, thinner ventricular walls and reduced trabeculation [Fig. 3A,B,E,F (controls) compared with 3C,D,G,H (eMYH knockdown hearts)]. Trabeculae appeared to be reduced in both size and number in the knockdowns harvested at HH19 (n=61), with all of the HH12/19 and HH16/19 (10 and 8, respectively), and 42 of 43 HH14/19 embryos affected, whereas none of the control embryos (n=83) had reduced trabeculation (Table 1). Stereological analysis showed that in controls the average percentage of the heart composed of ventricular wall and trabeculae was 20.38±1.10%, whereas in eMYH knockdown hearts this was reduced to 12.09±0.94%, a decrease of 40.66% (P=0.0001; n=9 for control or eMYH knockdown; numbers indicate average±s.e.m.).

Knockdown of eMYH leads to abnormal atrial septal development

Atrial septal development was analysed in embryos with eMYH knocked down at HH12 (prior to septa initiation), HH14 (around the stage of septa initiation) and HH16 (as the septum is growing) and harvested at HH19. The septa were noted to be abnormal in 60 out of 61 embryos in comparison with the control group, in which all except one heart showed normal septal development (n=83) (Table 2). The most severely affected hearts formed a small knuckle-shaped outgrowth from the dorsocranial atrial wall (Fig. 3C,G,J) and the less severely affected formed a normal-shaped septum that was reduced in size (Fig. 3D,H,K) in comparison with controls (Fig. 3A,B,E,F,I). At HH12/19, the septa were found to be knuckle-shaped in 8/10 of the knockdown embryos (80%; Fig. 3C) and the remaining embryos had a small septum (2/10; Fig. 3D,K). In HH14/19 hearts, a knuckle-shaped outgrowth was seen in 8 out of 43 (19%) and a small septum in 34 out of 43 embryos (79%; Fig. 3E-J). In one knockdown embryo, the septum appeared normal in size, although this embryo did have an enlarged heart. In HH16/19 embryos, 3 out of 8 (38%) had a knuckle-shaped septum and 5 out of 8 (62%) embryos had a small septum. HH14/17 control chicks, all presented with an atrial septum that showed natural variation in size as shown in Fig. 3L,M (n=14), whereas a septum was not observed in any of the eMYH knockdown hearts (n=16, Fig. 3N).

Stereological data (HH14/19) showed that control septa represented 1.19±0.43% (average±s.e.m.; n=9) of the heart, whereas in eMYH knockdown hearts the septa were just 0.29±0.11% of the heart (n=9; all classed as having a small septa), a decrease of 75.26% (P=0.04). Stereology showed no significant differences in endocardial cushions, atrial tissue, or wall or lumen sizes of the OFT and AVC. The HH14/17 stereology showed no significant differences within any of the tissue types counted (P>0.05; n=14 control, n=16 eMYH knockdown; stereological septal analysis was not possible owing to the small septum size at this stage).

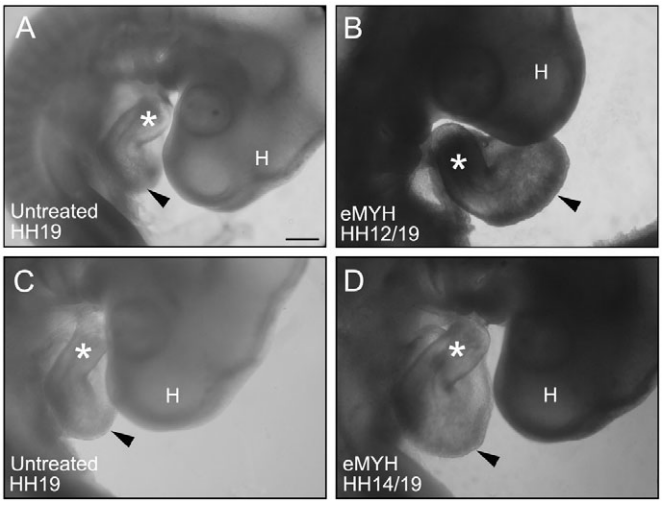

Fig. 2. eMYH knockdown leads to an enlarged heart in the chick. (**A-D**) Morpholino applied at HH12 (B) or HH14 (D), with harvesting at HH19 for eMYH knockdowns (B,D) and controls (A,C). External phenotypic analysis showed that eMYH knockdown embryos at HH12 (B) and HH14 (D) had an enlarged heart (arrowhead), in comparison with controls (A,C). Scale bar: 500 μm for all panels. H, head. Asterisk indicates outflow tract. Incubation periods: HH12, 50 hours; HH14, 54 hours; HH16, 57 hours; HH19, 81 hours.

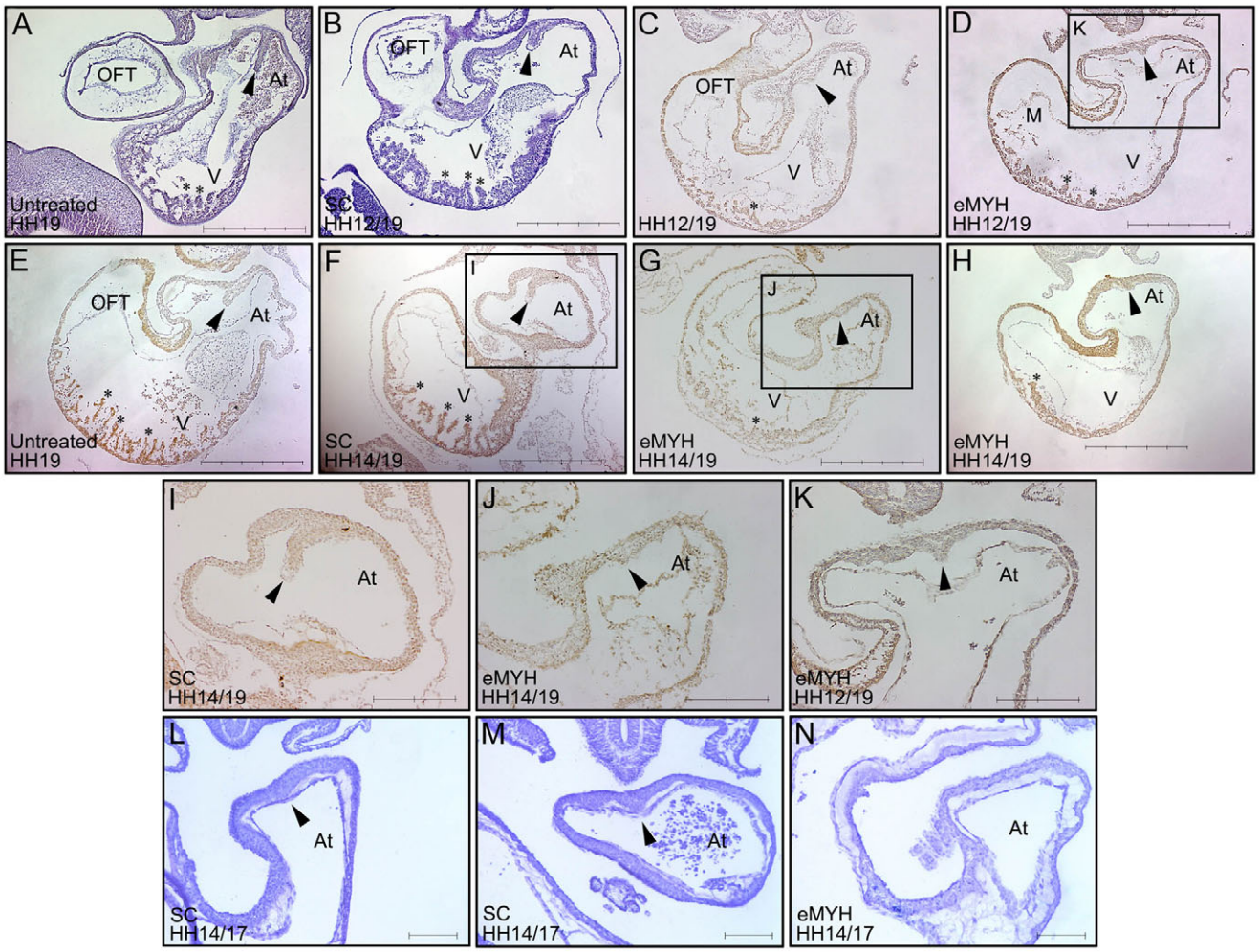

Fig. 3. Abnormal atrial and ventricular development upon eMYH knockdown. (**A-K**) Morpholino was applied at HH12 (B-D) or HH14 (F-H), with harvesting at HH19 for eMYH knockdowns (C,D,G,H) and controls (A,B,E,F). Knockdowns at HH12/19 (C,D) and 14/19 (G,H) had thinner ventricular walls and reduced trabeculae in comparison with controls (A,B,E,F). Abnormal atrial septa were seen in the knockdowns, with either a knuckle-shaped outgrowth (arrowheads in C,G,J) or normally shaped but reduced septa (arrowheads in D,H,K) compared with controls (arrowheads in A,B,E,F,I). From gross morphological phenotypic studies, hearts shown in A-F and H were normal in size whereas that shown in G was enlarged. I, J and K are enlarged views of the boxed areas in D, F and G, respectively. (**L-N**) Morpholino was applied at HH14 and tissue was harvested at HH17. HH14/17 controls (L,M) had stage-appropriate septa (arrowheads) and eMYH knockdowns (N) had no discernable septum. Scale bars: 500 μm for A-H; 200 μm for I-K; 100 μm for L-M; At, atrium; OFT, outflow tract; SC, standard control; V, ventricle. Asterisks indicate trabeculae. Incubation periods: HH12, 50 hours; HH14, 54 hours; HH16, 57 hours; HH17, 62 hours; HH19, 81 hours.

Electrical activity and calcium signalling are aberrant upon eMYH knockdown

Intracellular recordings of individual cardiomyocytes from spontaneously beating hearts (Arguello et al., 1986; Polo-Parada et al., 2009) in the presence of a morpholino (e-, α- or βMYH) at HH19 showed regional differences in the action potential (AP) phenotype in comparison with control hearts. Hearts treated with eMYH morpholino exhibited abnormal beating patterns characterised by absent or weak contractions, with a complete absence of AP in 75-80% of ventricular cells. However, electrically silent cells exhibited a large range of depolarised resting membrane potentials (Fig. 4E). Within the ventricular cells that did exhibit spontaneous APs, small amplitudes, long duration and slow rate of rise were observed compared with controls (Fig. 4B). By contrast, the atria displayed normal contractions and spontaneous APs, which were characterised by a decrease in amplitude and maximal rate of rise and an increase in duration (Fig. 4A). The long duration AP could be attributed at least in part to a decrease in I_K^+ (intracellular potassium) (Fig. 4F). Hearts treated with either α- or βMYH morpholino did not present any apparent differences in contraction or AP characteristics in either the atria or ventricles in comparison with controls (n=6 for α- or βMYH morpholino treated; Fig. 4A,B).

Ca^{2+} transients (increases in cytosolic Ca^{2+}) have previously been described in conjunction with AP in cardiomyocytes. Therefore, cytosolic Ca^{2+} was explored during the manipulation of e-, α- or βMYH in single isolated cells. Upon knockdown of eMYH, atrial cells displayed large variability in the duration of the Ca^{2+} transient, showing with some regularity a superimposition of a second or third maximal Ca^{2+} peak, and some small or aborted Ca^{2+} transient peaks (Fig. 4C). αMYH morpholino induced a modest change in Ca^{2+} transients, characterised in general by a low rise and decay with some small or aborted transients (Fig. 4C). βMYH morpholino-treated atrial cells showed irregular Ca^{2+}

Table 2. Summary of embryos with abnormal atrial septa formation

Stage†	Embryo type‡	Total	Atrial septation*		
			Knuckle	Small	Normal
HH12/19	Control	12	0	0	12
	eMYH knockdown	10	8	2	0
HH14/19	Control	58	0	0	58
	eMYH knockdown	43	8	34	1
HH16/19	Control	13§	0	1	12
	eMYH knockdown	8	3	5	0

*Qualitative assessment of atrial size obtained from serial histological sections.
†Stage of development when knockdown/harvesting were performed.
‡Control embryos include standard control, mismatch and untreated; eMYH denotes embryonic myosin heavy chain.
§One out of a total of 13 control embryos had a small heart and a reduced septum.

transient frequency, characterised mainly by superimposition of several spikes in a short period of time, inducing a large increase in Ca^{2+} levels (Fig. 4C). eMYH knockdown induced small changes in Ca^{2+} transient frequency in ventricular cells, characterised mainly by a moderate extension of the plateau phase in some of the Ca^{2+} transients observed (Fig. 4D). αMYH morpholino did not induce any appreciable change in Ca^{2+} transients in ventricular cells, whereas βMYH knockdown induced a decrease in the rise time during the Ca^{2+} transient and exhibited some small or aborted Ca^{2+} transients (Fig. 4D).

Sarcomeres are normal in eMYH knockdown hearts but tissue integrity is poor

Immunostaining and confocal microscopy of whole-mount heart preparations were performed to investigate eMYH knockdown effects at a subcellular level. Interestingly, the myofibrils (visualised with antibodies against sarcomeric α-actinin as a Z-disc protein) were relatively normal and no immature structures, such as premyofibrils, were observed (Rhee et al., 1994). The number of myofibrils per individual cell appeared comparable to controls. A subset of the cardiomyocytes showed completely diffuse staining for alpha-actinin (asterisk in Fig. 5); however, DAPI revealed that these were dividing cardiomyocytes in the process of disassembling their myofibrils (Ahuja et al., 2004). The cell-cell contact protein β-catenin also showed normal localisation around the plasma membrane of the cardiomyocytes (Hirschy et al., 2006) coupled with some nuclear signal. However, areas of poor tissue integrity were focally detected in all eMYH morpholino-treated hearts (arrows in Fig. 5C, compare with unaffected area in Fig. 5B; 4/12 eMYH morpholino-treated hearts were classified as moderately affected, 8/12 were severely affected), but were never observed in control hearts. To investigate whether other parts of the sarcomere were altered by eMYH knockdown, whole-mount preparations were also stained with antibodies against MyBP-C and EH-myomesin as markers for the A-band and M-band, respectively. Whereas the striations appeared indistinguishable from control cardiomyocytes, the disrupted tissue phenotype could again be observed (see Fig. S2A in the supplementary material). Electron microscopy also revealed poor tissue integrity but generally desmosomes, mitochondria and muscle fibres were comparable to controls in cells not undergoing apoptosis (see Fig. S2B in the supplementary material).

Reduced levels of eMYH did not affect cardiac proliferation

A total of 21,841 cells were identified as either PCNA positive (proliferating) or negative. In atria from control hearts, 57±10% (average percentage±s.e.m.) were PCNA positive, and in eMYH knockdown atria 54±6% cells were stained. In the septa, 45±3% positive cells were present in controls in comparison with 44±6% in eMYH knockdown tissue. The ventricles contained 64±17% PCNA-stained cells in controls in comparison with 70±2% in eMYH knockdowns. There were no significant differences between proliferation levels in either group in any of the regions analysed (P=0.8 for the atria and septa and P=0.7 for the ventricles).

Increased levels of apoptosis were observed following eMYH knockdown

A total of 9499 cells were identified as either apoptosis 'positive' or 'negative' in HH14/19 hearts (n=3 per group, average percentage±s.e.m.; see Fig. S3 in the supplementary material). Control atria showed 1.22±0.36% positive cells compared with 6.17±1.29% in knockdowns. In the septa, 0.87±0.44% positive cells were present in controls compared with 15.73±2.01% in eMYH knockdown samples. The ventricles contained 1.07±0.50% apoptotic cells in control hearts in comparison with 3.42±0.60% in eMYH knockdowns. The statistics indicate significant increases in apoptosis in eMYH knockdown hearts in comparison with controls in all regions analysed (P=0.002 septa, P=0.02 atria and P=0.04 ventricles, increases of 18%, 5% and 3%, respectively). The eMYH total cell numbers were decreased by 60% in the septa, 52% in the atria and 35% in the ventricles of eMYH knockdown chicks in comparison with controls.

Expression studies suggest human *MYH3* is the functional homologue of chick *eMYH*

RT-PCR was performed to compare the expression levels of the six human skeletal MYH genes present as a cluster on chromosome 17 (*MYH1*, *MYH2*, *MYH3*, *MYH4*, *MYH8* and *MYH13*). *MYH3* was the only gene expressed in the human foetal and adult heart (see Fig. S4 in the supplementary material). In situ hybridisation confirmed that *MYH3* was localised to atrial and ventricular myocardial walls, and skeletal muscle around ribs and bronchioles in 4, 5.5 and 7 week human embryos (Fig. 6A-F), with similar expression in E11.5 mouse embryo (Fig. 6G,H).

DISCUSSION

Embryonic MYH has a role in skeletal muscle development (Lagrutta et al., 1989; Lyons et al., 1990; Tajsharghi et al., 2008). Data presented here demonstrates that eMYH is also expressed during early cardiogenesis and plays a role in heart development.

The expression patterns of both α- and βMYH have been described previously in the developing chick. αMYH is predominately expressed in the atrium and atrial septum and is expressed at lower levels in the developing ventricular chambers

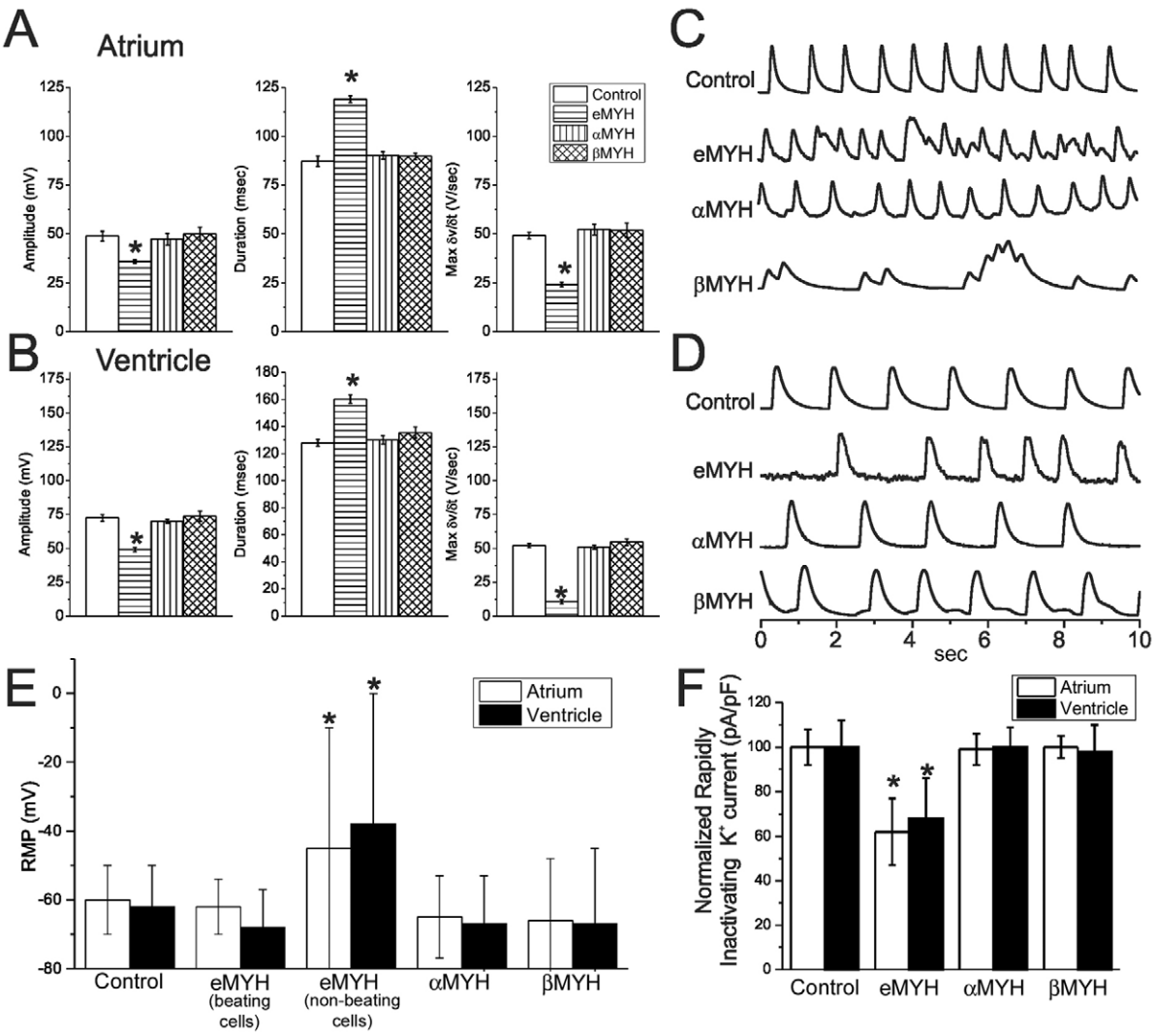

Fig. 4. Changes in cardiac action potential, intracellular Ca^{2+} and I_K^+ in vivo and in vitro in e-, α- and βMYH knockdowns. (**A**,**B**) Characteristics of action potentials from single cardiomyocytes from the atrium (A) or ventricle (B) of spontaneous beating hearts of controls (*n*=58 atria, 69 ventricles) or eMYH (*n*=24 atria, 22 ventricles), αMYH (*n*=31 atria, 28 ventricles) or βMYH (*n*=32 atria, 36 ventricles) knockdowns. (**C**,**D**) Changes in intracellular Ca^{2+} levels in spontaneous single isolated knockdown cells from the atrium (C) and ventricle (D). (**E**) Resting membrane potential (RMP) from atrial and ventricular cells of control (*n*=32 atria, 47 ventricles), eMYH beating (*n*=24 atria, 26 ventricles) and non-beating (*n*=43 atria, 38 ventricles) cells and αMYH- (*n*=22 atria, 26 ventricles) and βMYH- (*n*=16 atria, 25 ventricles) treated cells. (**F**) Rapidly inactivating K^+ current normalised to the mean of the I_K^+ control from atrial and ventricular cells, respectively (*n*=36 atria, 45 ventricles), and eMYH- (only spontaneous beating cells; *n*=52 atria, 65 ventricles), αMYH- (*n*=32 atria, 34 ventricles) and βMYH- (*n*=17 atria, 22 ventricles) treated cells. Error bars represent mean±s.e.m. *P<0.01.

(Rutland et al., 2009; Somi et al., 2006). Though initially expressed throughout the heart tube, βMYH becomes predominate in the ventricular myocardium as development proceeds (Somi et al., 2006). By comparison, expression of eMYH was demonstrated in the early looping heart, and subsequently throughout the myocardium of the OFT, atrium and atrial septum, and at lower levels to the ventricular chamber. Knockdown of eMYH in the chick resulted in abnormal atrial septal development, similar to that seen upon αMYH knockdown (Ching et al., 2005; Rutland et al., 2009). The atrial septum either failed to form with only a small outgrowth of the dorsocranial wall observed or a small septum formed in comparison with controls. Knockdown at different stages of septal development (HH12-HH16) showed no temporal effect with the phenotypes present at high penetrance (98% of eMYH knockdown embryos affected). In addition, there was an absent atrial septum in the HH14/17 knockdown hearts (only about 8 hours between knockdown and harvesting). Together, these data suggest that eMYH plays a specific and crucial role in atrial septa initiation and maintenance. Although the role eMYH plays in atrial septal formation is not fully understood, the 18% increase in apoptosis in the eMYH knockdown hearts suggests that eMYH might aid cell survival. Knockdown of eMYH also resulted in an enlarged heart and reduced trabeculation; however, no effect was observed upon myofibril assembly or maintenance. The enlarged external ventricular phenotype was observed in 82% and reduced trabeculae in 98% of eMYH knockdown hearts, with stereology indicating that the ventricular wall and trabeculae together were just 69% of the expected value. As the ventricle was enlarged but the wall was thinner, it was deemed appropriate to define the HH19 enlarged heart as dilated cardiomyopathy (Maron et al., 2006). This

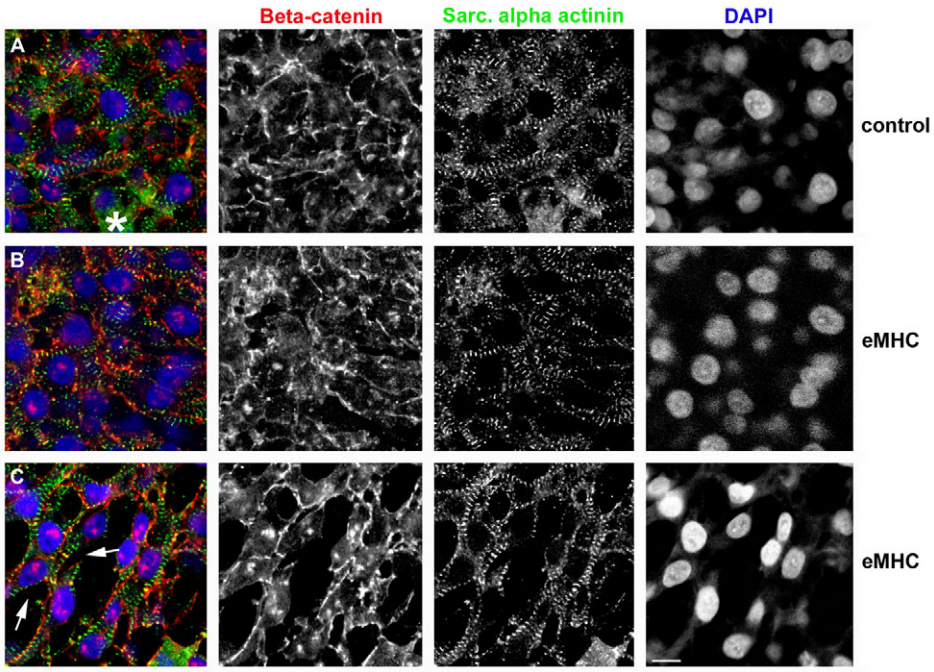

Fig. 5. The sarcomeres appear to form normally upon eMYH knockdown although the heart tissue has myocyte loss. (**A-C**) Confocal micrographs of HH19 whole-mount control (A) and eMYH-treated (B,C) hearts show β-catenin-labelled cell borders (second column, red signal in overlay) and sarcomeric alpha-actinin-labelled Z-discs (third column, green in overlay) and DAPI-stained nuclei (fourth column, blue signal in overlay). B shows an unaffected area and C shows tissue disintegration (arrows). Asterisk denotes dividing cell with disassembled myofibrils. Scale bar: 10 μm.

phenotype is also consistent with the increased tissue disintegration seen in subcellular analysis of embryonic heart structure and by an increase in apoptosis in eMYH knockdowns compared with controls. Apoptosis has previously been associated with dilated cardiomyopathy in humans and animal models during development and in the adult (Das et al., 2010; Guerra et al., 1999; Tintu et al., 2009; Wencker et al., 2003) and is potentially a mechanism in this disease (Wencker et al., 2003). Therefore, it was not unexpected that apoptosis was observed in these eMYH knockdown enlarged hearts. Data presented in Fig. 5 suggests that eMYH knockdown does not affect myofibrillogenesis or myofibril maintenance per se but results in focal impaired tissue integrity in the heart. These data might be explained by the expression of eMYH in a subset of the cardiomyocytes and its expression at the plasma membrane, suggesting a stabilising role in the cytoskeleton (Fig. 1C).

Many different mutations in *MYH7* (human analogue of β*MYH*) are known to cause cardiomyopathy (Walsh et al., 2010), with different mutations also associated with skeletal muscle myopathies (Meredith et al., 2004; Tajsharghi et al., 2003). In addition, some families with mutations in *MYH7* have both cardiomyopathy and myopathy (Tajsharghi et al., 2007), and mutations have been associated with cardiomyopathy in infants and children (Towbin et al., 2006). Both *MYH7* and *MYH6* (human homologue of α*MYH*) are known to be involved in normal atrial septal development, with families with mutations in these genes afflicted with ASDs (Budde et al., 2007; Ching et al., 2005). Furthermore, mutations in *MYH6* have also been found in individuals with cardiomyopathy (Carniel et al., 2005). Interestingly, mutations in the structural protein cardiac α-actin have been associated with atrial septal defects (Matsson et al., 2008) or cardiomyopathy (Mogensen et al., 1999; Olson et al., 2000; Olson et al., 1998), with some individuals with mutations having both defects (Monserrat et al., 2007). To our knowledge, *MYH3* or *eMYH* have not previously been associated with heart abnormalities in humans or animal models. The data presented here demonstrates that *MYH3* is the only skeletal MYH gene family member expressed in the human foetal heart, expressed in both the atrial and ventricular regions. Mutations in *MYH3* have been associated with distal arthrogryposis type I, 2A (Freeman-Sheldon syndrome) and 2B (Sheldon-Hall syndrome) (Alvarado et al., 2011; Toydemir et al., 2006). Mutations are largely missense, and are primarily to the head domain, potentially affecting the catalytic activity of *MYH3*. However, in many cases the consequence of a gene mutation is poorly understood. Therefore, different types of mutations might lead to different defects, such as ASDs with certain mutations and cardiomyopathy or skeletal myopathies with other mutations. Knockdown of chick eMYH leads to haploinsufficiency and, hence, a loss of function.

The excitation-contraction coupling process is fundamental to heart physiology: the electrical stimulus is usually an AP and the mechanical response is a contraction. The vast majority of papers on cardiac excitation-contraction coupling deal only with the ventricle (Fabiato and Fabiato, 1979; Langer, 1973; Orchard and Brette, 2008). In this study, we have shown the differing effects following the manipulation of e-, α- or βMYH in both the atria and ventricle at early stages of heart development, which might result in alterations between the generation of the electrical activity of the cells and their Ca^{2+} transients. These Ca^{2+} transient changes are fundamental to proper activation of the machinery of contraction, in which MYH plays a key role (Chandra et al., 2007; Dillmann, 2009; Khait and Birla, 2009), but also to the regulation of gene expression (Webb and Miller, 2003). Evidence is presented suggesting that eMYH has a major impact on the AP properties of the atrial and ventricular cells, with AP characteristics that are normally found during very early heart development (Arguello et al., 1986). These data suggest that eMYH might play a key role in the normal development of the AP in these regions. Some of the AP changes in eMYH-treated cells (such as the prolongation of the AP duration) resemble phenotypes described in NKX2.5- (Briggs et al., 2008; Pashmforoush et al., 2004) and TBX5- (Bruneau et al., 2001) deficient mice (which also exhibit atrial septal and conduction defects) or humans with heart failure (Kaab et al., 1998). Thus, it could be possible that eMYH knockdown alters these and/or other common proteins/pathways (such as the reducing potassium channel proteins Kv1.2, Kv1.5 and Kv2.1)

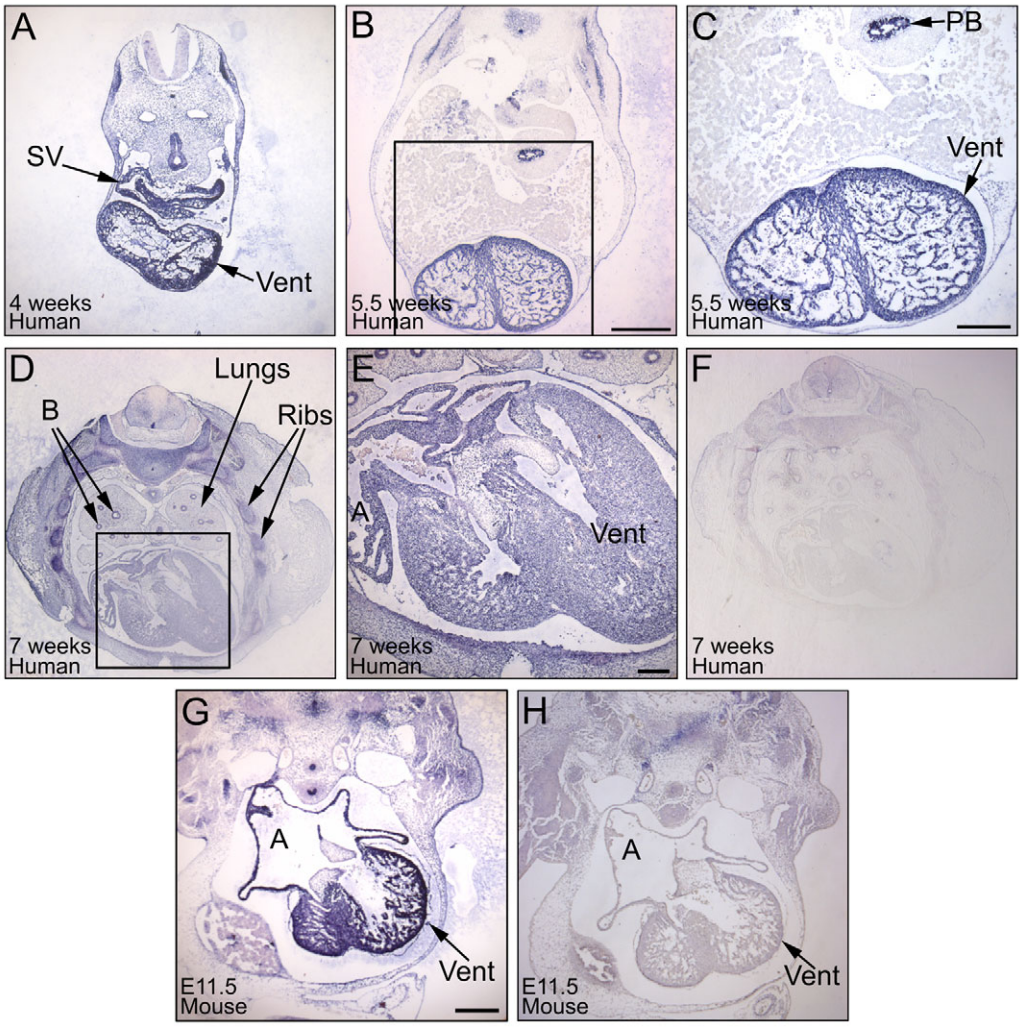

Fig. 6. In situ hybridisation of human *MYH3* on human and mouse foetal tissues. (**A-H**) *MYH3* in situ hybridisation on human 4 (A), 5.5 (B,C) and 7 (D-F) week foetal and E11.5 mouse (G,H) sections, with antisense (A-E,G) and sense negative control (F,H) probes. *MYH3* is present in the ventricle (Vent) and sinus venosus (SV) at 4 weeks (A). At 5.5 weeks, *MYH3* is observed in the ventricle, primary bronchus skeletal muscle (PB) (B,C) and in the atrium, ventricle and skeletal muscle around ribs and bronchi (B) at 7 weeks (D,E). C and E show enlarged views of the boxed areas in B and D, respectively. (G) In the E11.5 mouse embryo, *MYH3* is visualised in the atrium (A) and ventricle. Scale bars: 5 μm for A,B,D,F-H ; 2.5 μm for C,E.

resulting in similar phenotypes. Alternatively, changes in the mechanical forces in these altered hearts might result in a different microenvironment for the cardiomyocytes inducing a re-differentiation or de-differentiation process in these cells (Porter and Turner, 2009; Schenke-Layland et al., 2008). Furthermore, neither αMYH nor βMYH knockdown had a major impact in the AP morphology from the atria or ventricles. We found that a decrease in eMYH expression induces a disruption not only in the contraction of these cells but also in their ability to generate an AP, decreased I_K^+ and Ca^{2+} transient spikes (in ~80% of the ventricular myocytes). One possible explanation is that these electrically inactive cells represent ventricular cells that will undergo apoptosis, which is supported by the increase in apoptotic cells in the eMYH knockdown ventricles in comparison with controls. If this is the case, it raises new questions: Why are ventricular cells more sensitive than atrial cells? Is this a sign that early in development the excitation-contraction mechanism is tightly interrelated? If so, at what point in development does this interrelation become looser? Our current understanding of these issues is limited and further insights are required. Changes in the flow or load to the embryonic heart results in alterations in the composition and function of the cardiac microenvironment, modifying size, structure and function (Porter and Turner, 2009). Thus, the effects observed by eMYH reduction could be attributed to some of these factors.

It is recognised that intracellular Ca^{2+} plays a key role in the proper contraction of cardiomyocytes (Rigoard et al., 2009). In this study, we show that manipulation of e-, α- and βMYH have an impact on the profile of the spontaneous Ca^{2+} transients in atrial and ventricular cells. To what extent these changes in intracellular Ca^{2+} might affect the ability of cardiomyocytes to generate the proper force remains to be analysed. It is also well established that intracellular Ca^{2+} plays an important role not only in the contraction process but also in the modulation of many Ca^{2+} dependent intracellular functions. It remains to be elucidated whether the changes induced by manipulation of different MYHs are sufficient to temporarily or permanently alter any of these processes.

The data presented here demonstrates that eMYH is present in the early developing heart, and that it plays crucial roles during cardiogenesis, specifically in atrial septation and in normal heart function. Novel insights into the role that the MYH family plays in the electrical activity and calcium signalling within the developing heart are presented. These data suggest that the human functional homologue to *eMYH*, which we postulate to be *MYH3*, could provide novel insights into the molecular genetics of cardiovascular disorders and, hence, would be a candidate gene worthy of further investigation.

Acknowledgements
The authors would like to thank Sue Willington, Arjun Khurana and Dr Sue Chan for excellent technical assistance and Dr Paul Scotting for helpful discussions. We also thank the Advanced Microscopy Unit (Biomedical Sciences, University of Nottingham) and Mr Trevor Grey (Queen's Medical Centre, Nottingham). The EB165 antibody developed by Professor Bandman was obtained from the Developmental Studies Hybridoma Bank developed under the auspices of the NICHD and maintained by the University of Iowa, Department of Biology, Iowa City, IA 52242. Human embryonic material was provided by the Human Developmental Biology Resource (www.hdbr.org) which is supported by the MRC [G0700089] and the Wellcome Trust [082557]. This work was supported by British Heart Foundation (PG/06/021/20345 to S.L.) and American Heart Association (AHA-SDG0530140N to L.P.-P.) grants.

Competing interests statement
The authors declare no competing financial interests.

Supplementary material
Supplementary material for this article is available at
http://dev.biologists.org/lookup/suppl/doi:10.1242/dev.059063/-/DC1

References

Agarkova, I., Auerbach, D., Ehler, E. and Perriard, J. C. (2000). A novel marker for vertebrate embryonic heart, the EH-myomesin isoform. *J. Biol. Chem.* **275**, 10256-10264.
Ahuja, P., Perriard, E., Perriard, J. C. and Ehler, E. (2004). Sequential myofibrillar breakdown accompanies mitotic division of mammalian cardiomyocytes. *J. Cell Sci.* **117**, 3295-3306.
Alvarado, D. M., Buchan, J. G., Gurnett, C. A. and Dobbs, M. B. (2011). Exome sequencing identifies an MYH3 mutation in a family with distal arthrogryposis type 1. *J. Bone Joint Surg. Am.* **93**, 1045-1050.
Arguello, C., Alanis, J., Pantoja, O. and Valenzuela, B. (1986). Electrophysiological and ultrastructural study of the atrioventricular canal during the development of the chick embryo. *J. Mol. Cell Cardiol.* **18**, 499-510.
Bellairs, R. and Osmond, M. (1998). *The Atlas of Chick Development*. London, UK: Academic Press.
Ben-Shachar, G., Arcilla, R. A., Lucas, R. V. and Manasek, F. J. (1985). Ventricular trabeculations in the chick embryo heart and their contribution to ventricular and muscular septal development. *Circ. Res.* **57**, 759-766.
Briggs, L. E., Takeda, M., Cuadra, A. E., Wakimoto, H., Marks, M. H., Walker, A. J., Seki, T., Oh, S. P., Lu, J. T., Sumners, C. et al. (2008). Perinatal loss of Nkx2-5 results in rapid conduction and contraction defects. *Circ. Res.* **103**, 580-590.
Bruneau, B. G., Nemer, G., Schmitt, J. P., Charron, F., Robitaille, L., Caron, S., Conner, D. A., Gessler, M., Nemer, M., Seidman, C. E. et al. (2001). A murine model of Holt-Oram syndrome defines roles of the T-box transcription factor Tbx5 in cardiogenesis and disease. *Cell* **106**, 709-721.
Budde, B. S., Binner, P., Waldmuller, S., Hohne, W., Blankenfeldt, W., Hassfeld, S., Bromsen, J., Dermintzoglou, A., Wieczorek, M., May, E. et al. (2007). Noncompaction of the ventricular myocardium is associated with a de novo mutation in the beta-myosin heavy chain gene. *PLoS One* **2**, e1362.
Carniel, E., Taylor, M. R., Sinagra, G., Di, L. A., Ku, L., Fain, P. R., Boucek, M. M., Cavanaugh, J., Miocic, S., Slavov, D. et al. (2005). Alpha-myosin heavy chain: a sarcomeric gene associated with dilated and hypertrophic phenotypes of cardiomyopathy. *Circulation* **112**, 54-59.
Cerny, L. C. and Bandman, E. (1987). Expression of myosin heavy chain isoforms in regenerating myotubes of innervated and denervated chicken pectoral muscle. *Dev. Biol.* **119**, 350-362.
Chandra, M., Tschirgi, M. L., Ford, S. J., Slinker, B. K. and Campbell, K. B. (2007). Interaction between myosin heavy chain and troponin isoforms modulate cardiac myofiber contractile dynamics. *Am. J. Physiol. Regul. Integr. Comp. Physiol.* **293**, R1595-R1607.
Ching, Y. H., Ghosh, T. K., Cross, S. J., Packham, E. A., Honeyman, L., Loughna, S., Robinson, T. E., Dearlove, A. M., Ribas, G., Bonser, A. J. et al. (2005). Mutation in myosin heavy chain 6 causes atrial septal defect. *Nat. Genet.* **37**, 423-428.
Das, S., Babick, A. P., Xu, Y. J., Takeda, N., Rodriguez-Levya, D. and Dhalla, N. S. (2010). TNF-alpha-mediated signal transduction pathway is a major determinant of apoptosis in dilated cardiomyopathy. *J. Cell Mol. Med.* **14**, 1988-1997.
Davies, M. P., An, R. H., Doevendans, P., Kubalak, S., Chien, K. R. and Kass, R. S. (1996). Developmental changes in ionic channel activity in the embryonic murine heart. *Circ. Res.* **78**, 15-25.
Dillmann, W. (2009). Cardiac hypertrophy and thyroid hormone signaling. *Heart Fail. Rev.* **15**, 125-132.
Edgar, R. C. (2004). MUSCLE: multiple sequence alignment with high accuracy and high throughput. *Nucleic Acids Res.* **32**, 1792-1797.
Ehler, E., Rothen, B. M., Hammerle, S. P., Komiyama, M. and Perriard, J. C. (1999). Myofibrillogenesis in the developing chicken heart: assembly of Z-disk, M-line and the thick filaments. *J. Cell Sci.* **112**, 1529-1539.
Fabiato, A. and Fabiato, F. (1979). Calcium and cardiac excitation-contraction coupling. *Annu. Rev. Physiol.* **41**, 473-484.
Gonzalez-Sanchez, A. and Bader, D. (1985). Characterization of a myosin heavy chain in the conductive system of the adult and developing chicken heart. *J. Cell Biol.* **100**, 270-275.
Guerra, S., Leri, A., Wang, X., Finato, N., Di Loreto, C., Beltrami, C. A., Kajstura, J. and Anversa, P. (1999). Myocyte death in the failing human heart is gender dependent. *Circ. Res.* **85**, 856-866.
Guindon, S. and Gascuel, O. (2003). A simple, fast, and accurate algorithm to estimate large phylogenies by maximum likelihood. *Syst. Biol.* **52**, 696-704.
Gulick, J., Kropp, K. and Robbins, J. (1987). The developmentally regulated expression of two linked myosin heavy-chain genes. *Eur. J. Biochem.* **169**, 79-84.
Hamburger, V. and Hamilton, H. L. (1951). A series of normal stages in the development of the chick embryo. *J. Exp. Morphol.* **88**, 49-92.
Hamill, O. P., Marty, A., Neher, E., Sakmann, B. and Sigworth, F. J. (1981). Improved patch-clamp techniques for high-resolution current recording from cells and cell-free membrane patches. *Pflugers Arch.* **391**, 85-100.
Hendrix, M. J. and Morse, D. E. (1977). Atrial septation. I. Scanning electron microscopy in the chick. *Dev. Biol.* **57**, 345-363.
Hirschy, A., Schatzmann, F., Ehler, E. and Perriard, J. C. (2006). Establishment of cardiac cytoarchitecture in the developing mouse heart. *Dev. Biol.* **289**, 430-441.
Kaab, S., Dixon, J., Duc, J., Ashen, D., Nabauer, M., Beuckelmann, D. J., Steinbeck, G., McKinnon, D. and Tomaselli, G. F. (1998). Molecular basis of transient outward potassium current downregulation in human heart failure: a decrease in Kv4.3 mRNA correlates with a reduction in current density. *Circulation* **98**, 1383-1393.
Kelberman, D., de Castro, S. C., Huang, S., Crolla, J. A., Palmer, R., Gregory, J. W., Taylor, D., Cavallo, L., Faienza, M. F., Fischetto, R. et al. (2008). SOX2 plays a critical role in the pituitary, forebrain, and eye during human embryonic development. *J. Clin. Endocrinol. Metab.* **93**, 1865-1873.
Khait, L. and Birla, R. K. (2009). Changes in gene expression during the formation of bioengineered heart muscle. *Artif. Organs* **33**, 3-15.
Lagrutta, A. A., McCarthy, J. G., Scherczinger, C. A. and Heywood, S. M. (1989). Identification and developmental expression of a novel embryonic myosin heavy-chain gene in chicken. *DNA* **8**, 39-50.
Langer, G. A. (1973). Heart: excitation-contraction coupling. *Annu. Rev. Physiol.* **35**, 55-86.
Lyons, G. E., Ontell, M., Cox, R., Sassoon, D. and Buckingham, M. (1990). The expression of myosin genes in developing skeletal muscle in the mouse embryo. *J. Cell Biol.* **111**, 1465-1476.
Machida, S., Matsuoka, R., Noda, S., Hiratsuka, E., Takagaki, Y., Oana, S., Furutani, Y., Nakajima, H., Takao, A. and Momma, K. (2000). Evidence for the expression of neonatal skeletal myosin heavy chain in primary myocardium and cardiac conduction tissue in the developing chick heart. *Dev. Dyn.* **217**, 37-49.
Machida, S., Noda, S., Takao, A., Nakazawa, M. and Matsuoka, R. (2002). Expression of slow skeletal myosin heavy chain 2 gene in Purkinje fiber cells in chick heart. *Biol. Cell* **94**, 389-399.
Maron, B. J., Towbin, J. A., Thiene, G., Antzelevitch, C., Corrado, D., Arnett, D., Moss, A. J., Seidman, C. E. and Young, J. B. (2006). Contemporary definitions and classification of the cardiomyopathies: an American Heart Association scientific statement from the Council on Clinical Cardiology, Heart Failure and Transplantation Committee; quality of care and outcomes research and functional genomics and translational biology interdisciplinary working groups; and Council on Epidemiology and Prevention. *Circulation* **113**, 1807-1816.
Matsson, H., Eason, J., Bookwalter, C. S., Klar, J., Gustavsson, P., Sunnegardh, J., Enell, H., Jonzon, A., Vikkula, M., Gutierrez, I. et al. (2008). Alpha-cardiac actin mutations produce atrial septal defects. *Hum. Mol. Genet.* **17**, 256-265.
Mayhew, T. M. (1991). The new stereological methods for interpreting functional morphology from slices of cells and organs. *Exp. Physiol.* **76**, 639-665.

Meredith, C., Herrmann, R., Parry, C., Liyanage, K., Dye, D. E., Durling, H. J., Duff, R. M., Beckman, K., de Visser, M., van der Graaff, M. M. et al. (2004). Mutations in the slow skeletal muscle fiber myosin heavy chain gene (MYH7) cause laing early-onset distal myopathy (MPD1). *Am. J. Hum. Genet.* **75**, 703-708.
Merrifield, P. A., Sutherland, W. M., Litvin, J. and Konigsberg, I. R. (1989). Temporal and tissue-specific expression of myosin heavy chain isoforms in developing and adult avian muscle. *Dev. Genet.* **10**, 372-385.
Mogensen, J., Klausen, I. C., Pedersen, A. K., Egeblad, H., Bross, P., Kruse, T. A., Gregersen, N., Hansen, P. S., Baandrup, U. and Borglum, A. D. (1999). Alpha-cardiac actin is a novel disease gene in familial hypertrophic cardiomyopathy. *J. Clin. Invest.* **103**, R39-R43.
Mogensen, J., Perrot, A., Andersen, P. S., Havndrup, O., Klausen, I. C., Christiansen, M., Bross, P., Egeblad, H., Bundgaard, H., Osterziel, K. J. et al. (2004). Clinical and genetic characteristics of alpha cardiac actin gene mutations in hypertrophic cardiomyopathy. *J. Med. Genet.* **41**, e10.
Molina, M. I., Kropp, K. E., Gulick, J. and Robbins, J. (1987). The sequence of an embryonic myosin heavy chain gene and isolation of its corresponding cDNA. *J. Biol. Chem.* **262**, 6478-6488.
Monserrat, L., Hermida-Prieto, M., Fernandez, X., Rodriguez, I., Dumont, C., Cazon, L., Cuesta, M. G., Gonzalez-Juanatey, C., Peteiro, J., Alvarez, N. et al. (2007). Mutation in the alpha-cardiac actin gene associated with apical hypertrophic cardiomyopathy, left ventricular non-compaction, and septal defects. *Eur. Heart J.* **28**, 1953-1961.
Morse, D. E. (1978). Scanning electron microscopy of the developing septa in the chick heart. *Birth Defects Orig. Artic. Ser.* **14**, 91-107.
Niimura, H., Patton, K. K., McKenna, W. J., Soults, J., Maron, B. J., Seidman, J. G. and Seidman, C. E. (2002). Sarcomere protein gene mutations in hypertrophic cardiomyopathy of the elderly. *Circulation* **105**, 446-451.
Oana, S., Machida, S., Hiratsuka, E., Furutani, Y., Momma, K., Takao, A. and Matsuoka, R. (1998). The complete sequence and expression patterns of the atrial myosin heavy chain in the developing chick. *Biol. Cell* **90**, 605-613.
Olson, T. M., Michels, V. V., Thibodeau, S. N., Tai, Y. S. and Keating, M. T. (1998). Actin mutations in dilated cardiomyopathy, a heritable form of heart failure. *Science* **280**, 750-752.
Olson, T. M., Doan, T. P., Kishimoto, N. Y., Whitby, F. G., Ackerman, M. J. and Fananapazir, L. (2000). Inherited and de novo mutations in the cardiac actin gene cause hypertrophic cardiomyopathy. *J. Mol. Cell Cardiol.* **32**, 1687-1694.
Orchard, C. and Brette, F. (2008). t-Tubules and sarcoplasmic reticulum function in cardiac ventricular myocytes. *Cardiovasc. Res.* **77**, 237-244.
Pashmforoush, M., Lu, J. T., Chen, H., Amand, T. S., Kondo, R., Pradervand, S., Evans, S. M., Clark, B., Feramisco, J. R., Giles, W. et al. (2004). Nkx2-5 pathways and congenital heart disease; loss of ventricular myocyte lineage specification leads to progressive cardiomyopathy and complete heart block. *Cell* **117**, 373-386.
Polo-Parada, L., Zhang, X. and Modgi, A. (2009). Cardiac cushions modulate action potential phenotype during heart development. *Dev. Dyn.* **238**, 611-623.
Porter, K. E. and Turner, N. A. (2009). Cardiac fibroblasts: at the heart of myocardial remodeling. *Pharmacol. Ther.* **123**, 255-278.
Quiring, D. P. (1933). The development of the sino-atrial region of the chick heart. *J. Morphol.* **55**, 81-118.
Reiser, P. J., Portman, M. A., Ning, X. H. and Schomisch Moravec, C. (2001). Human cardiac myosin heavy chain isoforms in fetal and failing adult atria and ventricles. *Am. J. Physiol. Heart Circ. Physiol.* **280**, H1814-H1820.
Rhee, D., Sanger, J. M. and Sanger, J. W. (1994). The premyofibril: evidence for its role in myofibrillogenesis. *Cell Motil. Cytoskel.* **28**, 1-24.
Rigoard, P., Bauche, S., Buffenoir, K., Giot, J. P., Faure, J. P., Scepi, M., Richer, J. P., Lapierre, F. and Wager, M. (2009). [The anatomical substrate of muscle contractility]. *Neurochirurgie* **55** (Suppl. 1), S69-S82.
Rutland, C., Warner, L., Thorpe, A., Alibhai, A., Robinson, T., Shaw, B., Layfield, R., Brook, J. D. and Loughna, S. (2009). Knockdown of alpha myosin heavy chain disrupts the cytoskeleton and leads to multiple defects during chick cardiogenesis. *J. Anat.* **214**, 905-915.
Sacks, L. D., Cann, G. M., Nikovits, W., Jr, Conlon, S., Espinoza, N. R. and Stockdale, F. E. (2003). Regulation of myosin expression during myotome formation. *Development* **130**, 3391-3402.
Schenke-Layland, K., Rhodes, K. E., Angelis, E., Butylkova, Y., Heydarkhan-Hagvall, S., Gekas, C., Zhang, R., Goldhaber, J. I., Mikkola, H. K., Plath, K. et al. (2008). Reprogrammed mouse fibroblasts differentiate into cells of the cardiovascular and hematopoietic lineages. *Stem Cells* **26**, 1537-1546.
Sedmera, D., Pexieder, T., Hu, N. and Clark, E. B. (1997). Developmental changes in the myocardial architecture of the chick. *Anat. Rec.* **248**, 421-432.
Sissman, N. J. (1970). Developmental landmarks in cardiac morphogenesis: comparative chronology. *Am. J. Cardiol.* **25**, 141-148.
Slater, G. S. and Birney, E. (2005). Automated generation of heuristics for biological sequence comparison. *BMC Bioinformatics* **6**, 31.
Somi, S., Klein, A. T., Houweling, A. C., Ruijter, J. M., Buffing, A. A., Moorman, A. F. and Van Den Hoff, M. J. (2006). Atrial and ventricular myosin heavy-chain expression in the developing chicken heart: strengths and limitations of non-radioactive in situ hybridization. *J. Histochem. Cytochem.* **54**, 649-664.
Tajsharghi, H., Thornell, L. E., Lindberg, C., Lindvall, B., Henriksson, K. G. and Oldfors, A. (2003). Myosin storage myopathy associated with a heterozygous missense mutation in MYH7. *Ann. Neurol.* **54**, 494-500.
Tajsharghi, H., Oldfors, A., Macleod, D. P. and Swash, M. (2007). Homozygous mutation in MYH7 in myosin storage myopathy and cardiomyopathy. *Neurology* **68**, 962.
Tajsharghi, H., Kimber, E., Kroksmark, A. K., Jerre, R., Tulinius, M. and Oldfors, A. (2008). Embryonic myosin heavy-chain mutations cause distal arthrogryposis and developmental myosin myopathy that persists postnatally. *Arch. Neurol.* **65**, 1083-1090.
Tintu, A., Rouwet, E., Verlohren, S., Brinkmann, J., Ahmad, S., Crispi, F., van Bilsen, M., Carmeliet, P., Staff, A. C., Tjwa, M. et al. (2009). Hypoxia induces dilated cardiomyopathy in the chick embryo: mechanism, intervention, and long-term consequences. *PLoS One* **4**, e5155.
Towbin, J. A., Lowe, A. M., Colan, S. D., Sleeper, L. A., Orav, E. J., Clunie, S., Messere, J., Cox, G. F., Lurie, P. R., Hsu, D. et al. (2006). Incidence, causes, and outcomes of dilated cardiomyopathy in children. *JAMA* **296**, 1867-1876.
Toydemir, R. M., Rutherford, A., Whitby, F. G., Jorde, L. B., Carey, J. C. and Bamshad, M. J. (2006). Mutations in embryonic myosin heavy chain (MYH3) cause Freeman-Sheldon syndrome and Sheldon-Hall syndrome. *Nat. Genet.* **38**, 561-565.
Walsh, R., Rutland, C., Thomas, R. and Loughna, S. (2010). Cardiomyopathy: a systematic review of disease-causing mutations in myosin heavy chain 7 and their phenotypic manifestations. *Cardiology* **115**, 49-60.
Wang, L. and Duff, H. J. (1997). Developmental changes in transient outward current in mouse ventricle. *Circ. Res.* **81**, 120-127.
Webb, S. E. and Miller, A. L. (2003). Calcium signalling during embryonic development. *Nat. Rev. Mol. Cell Biol.* **4**, 539-551.
Wencker, D., Chandra, M., Nguyen, K., Miao, W., Garantziotis, S., Factor, S. M., Shirani, J., Armstrong, R. C. and Kitsis, R. N. (2003). A mechanistic role for cardiac myocyte apoptosis in heart failure. *J. Clin. Invest.* **111**, 1497-1504.
Wessels, A., Vermeulen, J. L., Viragh, S., Kalman, F., Lamers, W. H. and Moorman, A. F. (1991). Spatial distribution of 'tissue-specific' antigens in the developing human heart and skeletal muscle. II. An immunohistochemical analysis of myosin heavy chain isoform expression patterns in the embryonic heart. *Anat. Rec.* **229**, 355-368.
Wessels, A., Anderson, R. H., Markwald, R. R., Webb, S., Brown, N. A., Viragh, S., Moorman, A. F. and Lamers, W. H. (2000). Atrial development in the human heart: an immunohistochemical study with emphasis on the role of mesenchymal tissues. *Anat. Rec.* **259**, 288-300.
Wessels, M. W. and Willems, P. J. (2010). Genetic factors in non-syndromic congenital heart malformations. *Clin. Genet.* **78**, 103-123.